

See discussions, stats, and author profiles for this publication at: <https://www.researchgate.net/publication/231269865>

# Vacuum pyrolysis mass spectrometry of Pittsburgh No. 8 coal: Comparison of three different, time-resolved techniques

ARTICLE *in* ENERGY & FUELS · JANUARY 1991

Impact Factor: 2.79 · DOI: 10.1021/ef00025a002

---

CITATIONS

21

---

READS

24

4 AUTHORS, INCLUDING:



Yongseung Yun

Institute for Advanced Engineering

53 PUBLICATIONS 323 CITATIONS

SEE PROFILE

# Articles

## Vacuum Pyrolysis Mass Spectrometry of Pittsburgh No. 8 Coal: Comparison of Three Different, Time-Resolved Techniques

Yongseung Yun and Henk L. C. Meuzelaar\*

Center for Micro Analysis and Reaction Chemistry, 214 EMRL, Bldg. 61, University of Utah, Salt Lake City, Utah 84112

Norbert Simmleit

Chemical and Biological Laboratory, Institut Fresenius, D-6204 Taunusstein-Neuhof, F.R.G.

Hans-Rolf Schulten

Department of Trace Analysis, Fachhochschule Fresenius, D-6200 Wiesbaden, F.R.G.

Received February 12, 1990. Revised Manuscript Received October 17, 1990

Three different vacuum pyrolysis mass spectrometry techniques, viz., pyrolysis-field ionization mass spectrometry, thermogravimetry/low voltage electron ionization mass spectrometry, and Curie-point pyrolysis-low voltage electron ionization mass spectrometry, were used to analyze samples of Pittsburgh No. 8 coal obtained from the Argonne National Laboratory Premium Coal Sample Program. The primary objective was to assess the effects of differences in experimental techniques and conditions, e.g., with regard to heating rates, pyrolysis methods, and soft ionization procedures (FI vs low voltage EI) on the mass spectral patterns. A second objective was to further characterize and study the pyrolysis behavior of Pittsburgh No. 8 coal. The results indicate that the distribution and the type of the primary pyrolysis products are largely independent of marked differences in heating rate ( $10^{-2}$ – $10^4$  K/s range) and sample size ( $2.5 \times 10^{-5}$  to  $5.0 \times 10^{-2}$  g range) as well as overall vacuum pyrolysis MS configurations and conditions used. All three vacuum pyrolysis MS techniques produce remarkably similar mass spectral patterns when analyzing Pittsburgh No. 8 coal. The results show that Pittsburgh No. 8 coal contains a significant amount of low temperature ( $<380$  °C) evolving "bitumen" consisting primarily of alkyl-substituted aromatic components. The bitumen evolution step is followed by partially overlapping "bulk pyrolysis" step characterized by the evolution of abundant hydroxy- and dihydroxy-substituted aromatic compounds, thought to be primarily derived from vitrinitic components. During the bitumen evolution step the average MW of the compounds increases with temperature while maintaining a relatively narrow distribution. By contrast, during the bulk pyrolysis step, the average MW tends to decrease while exhibiting a much broader distribution.

### Introduction

Pyrolysis is the first step in most thermally driven coal conversion and utilization processes and, as such, is known to exhibit a profound effect on the course of these processes.<sup>1,2</sup> For example, in fixed bed coal gasification, pyrolysis products constitute the main source of the tar distillate and the pyrolysis conditions may be assumed to largely determine the physical and chemical characteristics of the liquids obtained from a given feed coal. In pulverized coal combustion, pyrolysis ("devolatilization") can be shown to affect the yield and composition of volatiles as a function of time and temperature, which in turn determines the temperature profile in the combustor and consequently influences char burnout as well as the for-

mation of  $\text{SO}_x$  and  $\text{NO}_x$  pollutant emissions. Although many other important factors affect coal conversion processes, the key role of pyrolysis reactions in coal conversion and utilization processes is nowadays widely acknowledged.<sup>3,4</sup>

A broad range of measurement results has been reported on the pyrolysis of coal under different experimental conditions, e.g., using the well-known heated screen pyrolysis technique.<sup>1,5</sup> In many coal pyrolysis experiments, however, it has been difficult, if not impossible, to distinguish the effects of secondary reactions, e.g., due to mass-transfer limitations from the primary coal pyrolysis reactions. Pyrolysis under vacuum conditions can help to overcome these problems, provided sufficiently small

(1) Howard, J. B. In *Chemistry of Coal Utilization, Second Supplementary Volume*; Elliott, M. A., Ed.; Wiley: New York, 1981; pp 665-784.

(2) Nelson, P. F.; Smith, I. W.; Tyler, R. J.; Mackie, J. C. *Energy Fuels* 1988, 2, 391-400.

(3) Brewster, B. S.; Baxter, L. L.; Smoot, L. D. *Energy Fuels* 1988, 2, 362-370.

(4) Smith, J. D.; Smith, P. J.; Hill, S. C. Submitted for publication in *Comput. Chem. Eng.*

(5) Gavalas, G. R. *Coal Pyrolysis*; Elsevier: Amsterdam, 1982.

particle sizes and/or low heating rates are employed.<sup>6,7</sup> As a result, it has been proposed that mostly primary pyrolysis products are observed in vacuum micropyrolysis experiments.<sup>8</sup> In addition, time-resolved mass spectrometric analysis of vacuum pyrolysis products can yield detailed information about the temperature-dependent behavior of specific mass signals or grouped mass signals, which can be used to calculate kinetic parameters for coal pyrolysis models and/or devolatilization submodels.<sup>9</sup>

With the availability of eight Argonne National Laboratory Premium Coal Sample Program (ANL-PCSP) Coals, a systematic comparison of results obtained with different instruments and experimental conditions, and even by different research groups, on the same coals has become possible. Along these lines, the authors decided to use three different time-resolved pyrolysis mass spectrometry techniques for Pittsburgh No. 8 coal in order to study the characteristics of pyrolyzates as well as the distribution of the primary pyrolysis products as a function of time, temperature, and heating rate in addition to the effect of different ionization techniques. Another important objective for this study was to examine whether heating rate has a major effect on the mechanism of coal pyrolysis since many useful data on coal pyrolysis are obtained at low heating rates while most pyrolysis in real processes occurs at high heating rates ( $>10^4$  K/s). Changes in heating rate can be achieved by different types of heating methods: namely, laser pyrolysis ( $>10^4$  K/s), Curie-point induction heating ( $10^2$ – $10^4$  K/s), and electrical heating ( $<10$  K/s). Pyrolysis products are mainly analyzed by mass spectrometry in our study. The study including laser heating will be a subject of another paper. Thus the three techniques used were pyrolysis-field ionization mass spectrometry (Py-FIMS) at 100 K/min, Thermogravimetry/low voltage electron ionization mass spectrometry (TG/LVMS) at 2 and 25 K/min, and Curie-point pyrolysis-low voltage electron ionization mass spectrometry (Py-LVMS) at ca. 100 K/s.

### Experimental Section

Aliquots of a Pittsburgh No. 8 (–100 mesh) ANL-PCSP sample were analyzed under vacuum Py-FIMS, TG/LVMS, and Curie-point Py-LVMS conditions. While Py-FIMS and TG/LVMS techniques employed the original –100 mesh particle size without further grinding, the standard Py-LVMS technique required further ground (5–20  $\mu$ m) coal particles. Ultimate analysis data provided by Vorres et al.<sup>10</sup> are 75.5% C, 4.83% H, 1.49% N, 6.74% O (by difference), 2.19% S, and 9.25% ash (dry basis). More detailed petrographic, chemical, and physical analysis data can be found in ref 10.

**Pyrolysis-Field Ionization Mass Spectrometry (Py-FIMS).** The experimental setup of the Finnigan MAT FI ion source is shown in Figure 1a. About 100  $\mu$ g of coal was placed in a quartz crucible which was inserted into the high vacuum ( $10^{-7}$  Torr) of the ion source using an AMD Intra direct introduction system (Beckeln, FRG).<sup>11</sup> The crucible was heated from 50 to 730 °C at a linear heating rate of 100 K/min. The oven temperature was measured at the bottom of the crucible by using a thermocouple. Moreover, the ion source was maintained at a temperature of 200 °C. The tip of the AMD probe, the wall of

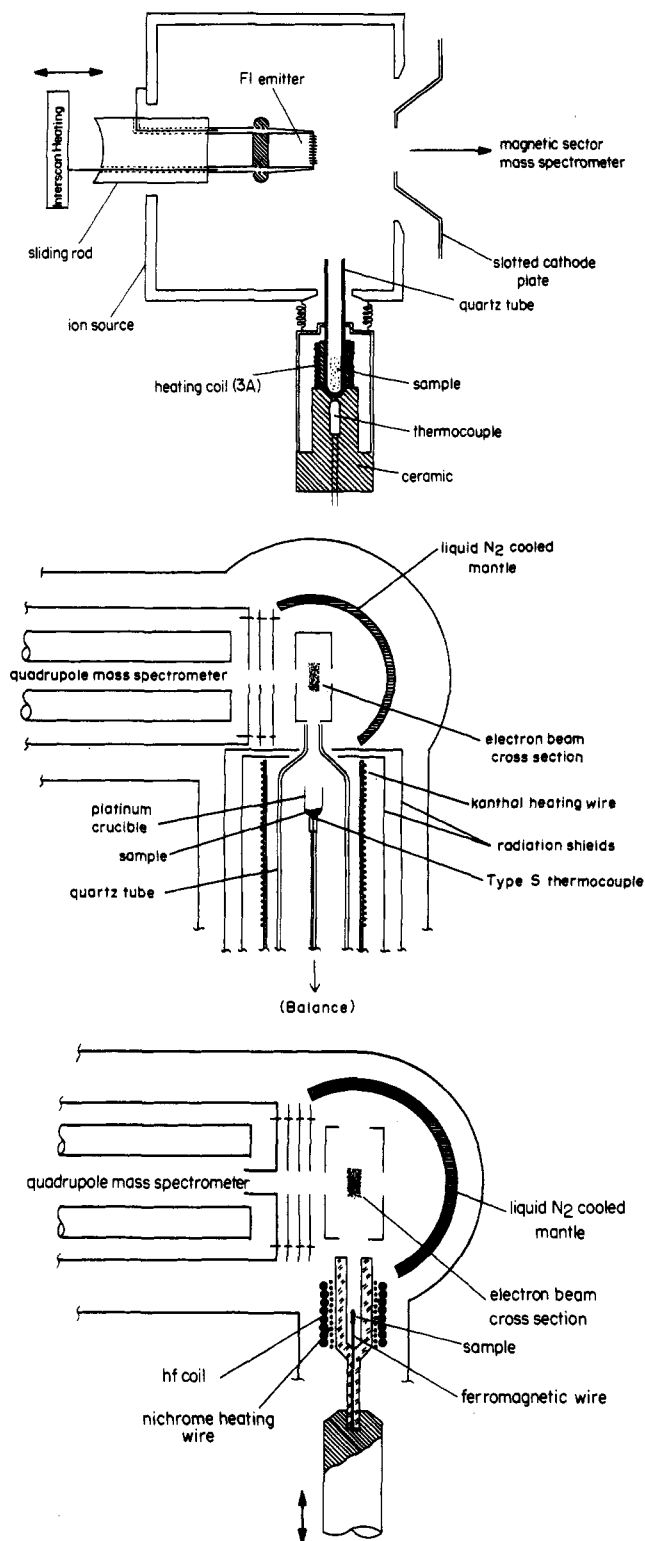


**Figure 1.** (a, top) Schematic diagram of Py-FIMS system. (b, middle) Schematic diagram of vacuum TG/LVMS system, based on the combination of a Mettler TA1 TG/DTA system and a Finnigan MAT 3200 quadrupole mass spectrometer with specially designed vacuum housing. (c, bottom) Schematic diagram of Curie-point Py-LVMS system.

the ionization chamber, and the FI emitter were held at the same electric potential of 8 kV. Emitters were prepared from 100- $\mu$ m tungsten wire which had been activated with benzonitrile at 1200 °C.<sup>12</sup> Thirty-four mass spectra were recorded for Pittsburgh No. 8 coal in the  $m/z$  50–900 mass range. Between repetitive scans

(6) Blik, A.; van Poelje, W. M.; van Swaaij, W. P. M.; van Beckum, F. P. M. *AIChE J.* **1985**, *31*(10), 1666–1681.

(7) Howard, J. B.; Peters, W. A.; Serio, M. A. EPRI Report No. AP-1803, EPRI: Palo Alto, CA, April 1981.

(8) Marzec, A. J. *Anal. Appl. Pyrolysis* **1985**, *8*, 241–254.

(9) Yun, Y.; Maswadeh, W.; Meuzelaar, H. L. C.; Simmleit, N.; Schulten, H.-R. *Prepr. Pap.—Am. Chem. Soc., Div. Fuel Chem.* **1989**, *34*(4), 1308–1316.

(10) Vorres, K. S. *Users Handbook for the Argonne Premium Coal Sample Program*.

(11) Schulten, H.-R.; Simmleit, N.; Müller, R. *Anal. Chem.* **1987**, *59*, 2903–2908.

(12) Schulten, H.-R.; Beckey, H. D. *Organic Mass Spectrom.* **1972**, *6*, 885–895.

the emitter was flash-heated to approximately 1500 °C in order to avoid condensation and to regenerate the surface of the emitter<sup>11</sup> thereby increasing overall reproducibility of the Py-FIMS profiles. The FIMS system was operated in nominal resolution mode. High-resolution operation is possible, as described elsewhere,<sup>13</sup> but is unfortunately not yet compatible with rapid time-resolved scanning used for obtaining the pyrolysis MS data discussed here.

**Thermogravimetry/Low Voltage Electron Ionization Mass Spectrometry (TG/LVMS).** The TG/LVMS system used (Figure 1b) consisted of a Mettler TA1 Thermoanalyzer directly interfaced to a small Finnigan MAT 3200 quadrupole mass filter. Pyrolysis was performed directly in front of the ion source of the mass spectrometer in order to prevent recombination reactions and/or secondary decomposition of reactive compounds as well as to minimize the loss of polar compounds through condensation. The distance from the center of the electron beam cross section to the top of the platinum crucible was 2 in. A quartz tube positioned between the heater wall and the platinum crucible prevented contamination of the heater and focuses pyrolysis products into the ion source. The quartz tube was cleaned after each experiment with a Bunsen burner. After several experiments, the ion source was also cleaned carefully. A turbomolecular pump (Balzer TPU 050) was used for evacuating the MS chamber up to  $4 \times 10^{-7}$  Torr in 7–8 min. In addition, two diffusion pumps were used to maintain a pressure of less than  $1 \times 10^{-4}$  Torr in the TG balance chamber. The liquid nitrogen cold trap in Figure 1b was used to ensure a low background signal level. Sample aliquots of 4–5 mg were placed in a 7 mm i.d., 11 mm high, round-bottom platinum crucible and heated under vacuum while the temperature was increased from ambient to 700 °C at 25 K/min, or from 200 to 445 °C at 2 K/min. The smaller temperature range of the slow heating run was chosen to cover the most important stages of coal devolatilization while accommodating the maximum time limit of the MS scan clock ( $\sim 2$  h). In the 2 K/min run, 50 mg of sample was used in order to maintain a sufficiently high signal level. MS conditions were as follows: electron ionization (set value) 14 eV, mass range scanned 50–195 amu (33–350 amu for higher mass range scans), total number of scans 80, total scan time 27 min (123 min for the higher mass scan run). Each spectrum scanned was recorded and stored separately by means of an IBM 9000 computer with specially built MS interface.

**Curie-Point Pyrolysis-Low Voltage Electron Ionization Mass Spectrometry (Py-LVMS).** Py-LVMS experiments were performed using an Extranuclear 5000-1 Curie-point Py-MS system with the specially designed inlet system shown in Figure 1c. The coal sample was hand ground into a fine, uniform suspension in Spectrograde methanol (5 mg of sample per milliliter of methanol). Average particle size was approximately 5–20  $\mu\text{m}$ . Five microliters of the suspension was coated on a 0.5 mm diameter ferromagnetic wire (Curie-point temperature 610 °C) and air-dried under continuous rotation for approximately 1 min, resulting in the deposition of approximately 25  $\mu\text{g}$  of dry coal sample on the wire. The coated wire was inserted into a borosilicate glass reaction tube, introduced into the vacuum system of the mass spectrometer, and inductively heated at a rate of approximately 100 K/s to the Curie-point temperature (610 °C). Total MS scan time was 8 s. A higher heating rate (approximately 1500 K/s, total heating time 0.4 s) was employed to evaluate the effect of heating rate on the spectra, e.g., for comparison with low heating rate TG/LVMS runs. During the high heating rate run, the radio frequency (rf) coil region was electrically preheated at 250 °C to reduce condensation losses of compounds in the borosilicate reaction tube. Other MS conditions were as follows: electron impact energy 12 eV, mass range scanned 50–200 amu, total number of scans 41, total scan time 15 s. The observed yield of fragment ions produced by electron ionization at 12 eV (set value) in the Py-LVMS system in terms of the intensity ratio of  $m/z$  106 /  $m/z$  91 from *m*-xylene was 2.64 whereas the intensity ratio of  $\text{N}_2^+/\text{O}_2^+$  from background air was 0.54. At 13.3 eV (set value) intensities from  $\text{N}_2^+$  and  $\text{O}_2^+$  were found to become identical.

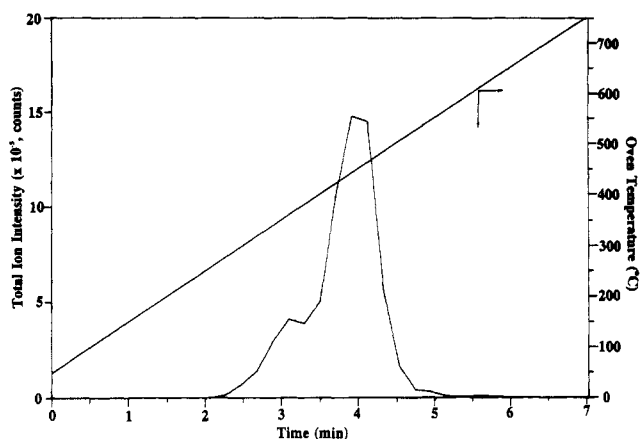


**Figure 2.** Temperature-time profile superimposed on the total ion intensity profile from Py-FIMS analysis.

Two time-integrated runs also were performed at heating rates of approximately 150 and  $6 \times 10^4$  K/s. Preheated temperatures for the rf coil region were 200 °C (150 K/s run) and 250 °C ( $6.0 \times 10^4$  K/s run). Mass range scanned was 33–210 amu and 100 scans were obtained. Other MS conditions are the same as described above.

## Results and Discussion

FIMS is known to produce minimal fragmentation of molecular ions and is generally considered to be one of the most promising techniques to obtain reliable molecular weight data on coal pyrolyzates. Response factors for aromatic and hydroaromatic compounds are reported to be nearly identical,<sup>14</sup> although response factors for aliphatic compounds may show relatively large variations.<sup>15</sup> In view of the fact that advanced coal devolatilization models such as the FG-DVC model developed by Solomon et al.<sup>16</sup> are able to predict MW distributions of the pyrolysis tars as a function of temperature, Py-FIMS techniques offer a promising approach toward model comparison and verification as well as estimation of important modeling parameters. In addition, high-resolution Py-FIMS has been shown to be highly useful for further defining the chemical composition of pyrolysis tars.<sup>13</sup>

Figure 2 illustrates the temperature profile employed in Py-FIMS as well as the total ion intensity (TII) profile. However, since temperatures are measured directly outside the quartz crucible, there may be some difference between actual sample temperature and measured temperature.<sup>17</sup> The TII profile clearly shows a bimodal distribution thought to represent the consecutive evolution of thermally extractable "bitumen" components and "bulk pyrolysis" components, respectively. In this paper we will refer to the first hump in the TII profile as the "thermally extractable bitumen" or simply "bitumen" and to the second, major hump as the "bulk pyrolyzate". The justification for this terminology will be discussed in subsequent paragraphs. If symmetrical evolution profiles are assumed for the two components, the early evolving bitumen components represent approximately 25% of the total pyrolyzate. Further, assuming equal average response factors for the various types of compounds in both humps, this indicates that the thermally extractable bitumen components ac-

(14) Scheppele, S. E.; Grizzle, P. L.; Greenwood, G. J.; Marriott, T. D.; Perrerrin, N. B. *Anal. Chem.* 1976, 48(14), 2105–2113.

(15) Scheppele, S. E.; Grindstaff, Q. G.; Grizzle, P. L. *Mass Spectrometric Characterization of Shale Oils*; Aczel, Thomas, Ed.; ASTM: Philadelphia, 1986; ASTM STP 902, pp 49–80.

(16) Solomon, P. R.; Hamblen, D. G.; Caragelo, R. M.; Serio, M. A.; Deshpande, G. V. *Energy Fuels* 1988, 2, 405–422.

(17) Schulten, H.-R. *J. Anal. Appl. Pyrolysis* 1987, 12, 149–186.

(13) Schulten, H.-R.; Marzec, A.; Dyla, P.; Simmleit, N.; Müller, R. *Energy Fuels* 1989, 3, 481–487.

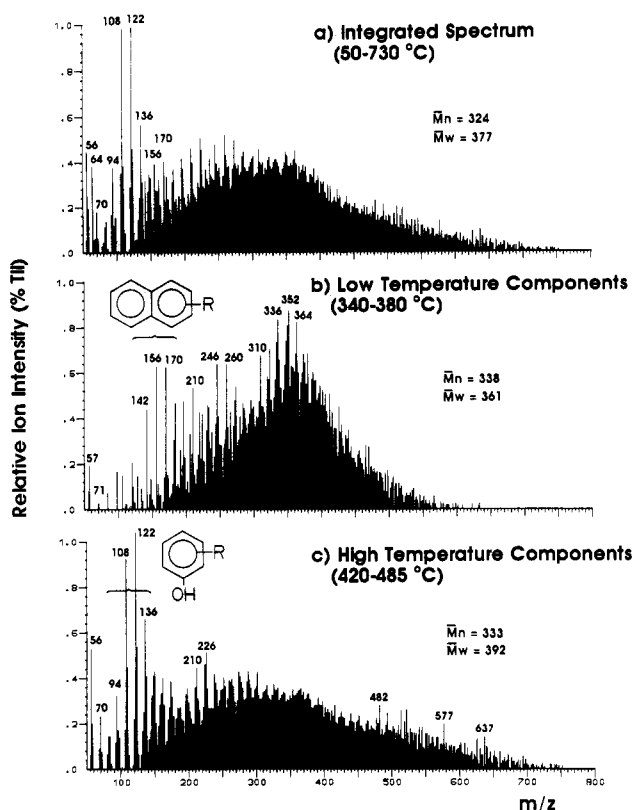


**Figure 3.** Comparison of Pittsburgh No. 8 coal Py-FI mass spectra recorded over different temperature intervals.

count for approximately 25% of the tar yield from Pittsburgh No. 8 coal. Total tar yield has been reported to be 30–35% (dry, ash free basis) for the Argonne Premium Pittsburgh No. 8 coal under the following experimental conditions: helium flow velocity 0.1 m/s, pressure 1.2 bar, final temperature 700 °C, holding time 30 s, heating rates from 1 to 1000 K/s.<sup>18</sup> Consequently, approximately 6–8% (w/w) of the original ANL-PCSP ampule sample can be considered as thermally extractable bitumen after corrections for moisture content (1.7%) and ash (9.1%). Since thermally extractable bitumen components by and large may be expected to constitute a subset of all true (i.e., solvent extractable) bitumen components, this percentage would seem to agree well with levels of toluene (5.7%) and tetrahydrofuran (12.3%) solubles for ANL-PCSP Pittsburgh No. 8 coal on an as-received basis reported by Buchanan et al.<sup>19</sup> and White.<sup>20</sup>

Vacuum pyrolyzates from Pittsburgh No. 8 coal contain a broad range of molecular sizes ranging from 2 to 800 amu. In Figure 3, Py-FIMS results covering the 50–750 amu range are illustrated. The most prominent mass peaks in the time-integrated (summation of all scans) spectrum, as illustrated in Figure 3a, are thought to represent alkyl-substituted phenols ( $m/z$  94, 108, 122, 136) known to be primarily derived from vitrinitic components in coal.<sup>21,22</sup> Considering the heterogeneity of coal, each mass signal is likely to contain contributions from several different ion species. Consequently, structural assignments mentioned in this paper are based on pyrolysis gas chromatogra-

phy/mass spectrometry (Py-GC/MS) data on Pittsburgh No. 8 coal (50–400 amu range), which indicate that more than 80% of a given mass signal is coming from the specified compound or series of homologues.

Inspection of mass spectra obtained over a specific temperature range also helps to interpret the chemical and physical characteristics of the tar components observed in Py-FIMS. The time-integrated spectrum of three scans around the maximum of the bitumen peak in Figure 2 is shown in Figure 3b. In addition, Figure 3c shows the time-integrated spectrum of the top four scans from the “bulk pyrolysis” peak. Mean number averaged and weight averaged MW’s of Pittsburgh No. 8 coal are 324 and 377, respectively, for the whole (50–730 °C) temperature range scanned as compared to 338 and 316, respectively, for the 340–380 °C range or 333 and 392, respectively, over the 420–485 °C range. In the low-temperature (bitumen) components, the most prominent series of homologous compounds represent primarily alkyl-substituted naphthalenes ( $m/z$  128, 142, 156, 170, 184), phenanthrenes ( $m/z$  178, 192, 206, 220, 234, 248), and several other homologous series, e.g., at  $m/z$  168, 182, 196, 210, 224, 238 (acenaphthenes and biphenyls) and  $m/z$  204, 218, 232, 246, 260, 274, 288 (e.g., phenylnaphthalenes) and  $m/z$  254, 268, 282, 296, 310, 324, 338 (e.g., naphthylphenanthrenes and phenylphenanthrenes). These tentative structural assignments are based on Py-GC/MS<sup>23</sup> and high-resolution Py-FIMS<sup>13</sup> results obtained on similar coals. Although some aliphatic components are observed at  $m/z$  56, 57, 70, 71, 84, 98, the main bitumen components appear to be (alkyl)aromatic in nature. It is also noteworthy that at lower temperature aliphatic  $C_nH_{2n+1}^+$  ion signals (e.g., at  $m/z$  57, 71) are more dominant than  $C_nH_{2n}^+$  ion signals (e.g., at  $m/z$  56, 70) while at higher temperatures the situation is reversed. This would seem to correspond to the observations of Nip et al.<sup>21</sup> and others of high alkane/alkene ratios at low temperatures vs alkane/alkene ratios <1 at true pyrolysis temperatures.

Among the high-temperature (bulk pyrolysis) components, alkyl-substituted phenols ( $m/z$  94, 108, 122, 136) and dihydroxybenzenes ( $m/z$  110, 124, 138) are dominant peaks in addition to alkene signals at  $m/z$  56, 70, 84, 98. Alkyl-substituted benzenes, naphthalenes, and phenanthrenes are also present, albeit at lower abundances than their hydroxy-substituted analogues. Other noticeable homologous series are thought to represent naphthols ( $m/z$  144, 158, 172, 186) and hydroxyindenes plus tetralins ( $m/z$  132, 146, 160, 174). Considering that the most prominent homologous series in high-temperature components of coals from lignite to high volatile bituminous rank are alkyl-substituted phenols and dihydroxybenzenes, thought to be derived from vitrinitic components in coal,<sup>22,24</sup> and considering that vitrinites represent 85 wt % (mmf) of Pittsburgh No. 8 coal, and further considering that the high-temperature components represent about 75% of the integrated TII, the term bulk pyrolyzates for the high-temperature components appears to be appropriate.

As shown in Figure 3, the narrow MW range of the low-temperature components is markedly different from the much broader MW range of the high-temperature components. Figure 4 provides a more detailed overview of MW distribution trends as a function of temperature. Note that FIMS intensities were summed over arbitrarily chosen mass ranges of 50 daltons. In the bitumen evolu-

(18) Gibbins-Matham, J.; Kandiyoti, R. *Energy Fuels* 1988, 2, 505–511.

(19) Buchanan, D. H.; Mai, W. *Prepr. Pap.—Am. Chem. Soc., Div. Fuel Chem.* 1987, 32(4), 293–300.

(20) White, R. Master's Thesis, University of Utah, 1989.

(21) Nip, M.; Tegelaar, E. W.; Brinkhuis, H.; de Leeuw, J. W.; Schenk, P. A.; Holloway, P. J. In *Advances in Organic Geochemistry, 1985*; Leythaeuser, D., Rullkötter, J., Eds.; *Org. Geochem.* 1986, 10, 769–778.

(22) Chakravarty, T.; Windig, W.; Hill, G. R.; Meuzelaar, H. L. C.; Khan, M. R. *Energy Fuels* 1988, 2, 400–405.

(23) Nip, M.; Genuit, W.; Boon, J. J.; de Leeuw, J. W.; Schenck, P. A.; Blazsó, M.; Székely, T. *J. Anal. Appl. Pyrolysis* 1987, 11, 125–147.

(24) Meuzelaar, H. L. C.; Harper, A. M.; Pugmire, R. J.; Karas, J. *Int. J. Coal Geol.* 1984, 4, 143–171.

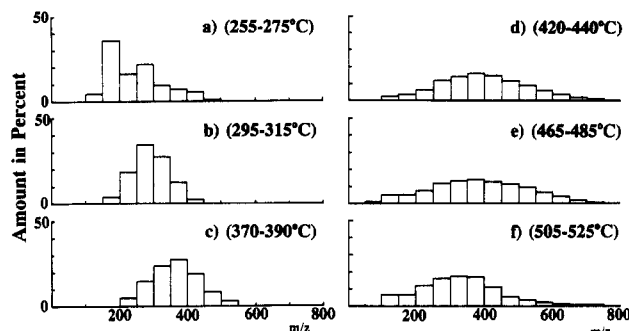


**Figure 4.** Molecular weight distributions of pyrolyzates in six successive temperature intervals during Py-FIMS analysis at 100 K/min. The FI signal intensities were added in arbitrarily chosen mass classes of 50 daltons.

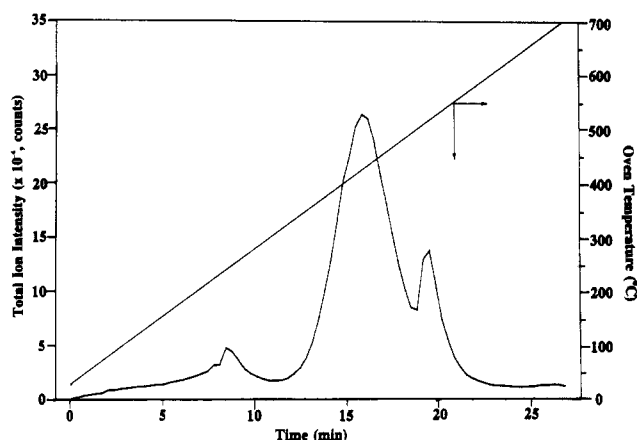


**Figure 5.** Temperature-time profile superimposed on the total ion intensity profile from TG/LVMS analysis.

tion step (parts a, b, and c in Figure 4), average MW increases with temperature while in the bulk pyrolysis step average MW decreases with temperature. The above observations support the hypothesis that the bitumen evolution step primarily represents desorption and distillation phenomena rather than pyrolysis events.<sup>22</sup> Moreover, the transition between steps c and d in Figure 4 is rather abrupt, suggesting that the two processes of bitumen evolution and bulk pyrolysis are relatively independent of each other. Consequently, at least two sets of kinetic parameters are necessary to describe the whole vacuum devolatilization process of Pittsburgh No. 8 coal and comprehensive coal devolatilization models should take this into account. The implications of the observed phenomena for the ongoing discussions about the putative "mobile phase" in coal are examined in a separate publication.<sup>25</sup>

The temperature vs time profile employed in TG/LVMS and the resulting TII profile for Pittsburgh No. 8 coal are shown in Figure 5. As can be seen in Figure 1b, the temperature measured in the TG/LVMS experiment is the temperature of the platinum crucible which may be slightly different from the actual sample temperature. The TG/LVMS TII profile reveals no less than three distinct humps. The first and second humps represent the low-temperature bitumen evolution step and bulk pyrolysis step, respectively, as also observed in Py-FIMS. In addition, the third hump corresponds to the decomposition of pyrite into pyrrhotite, characterized by greatly increased intensities at  $m/z$  64 ( $S_2^+$  and perhaps some  $SO_2^+$ ). In the

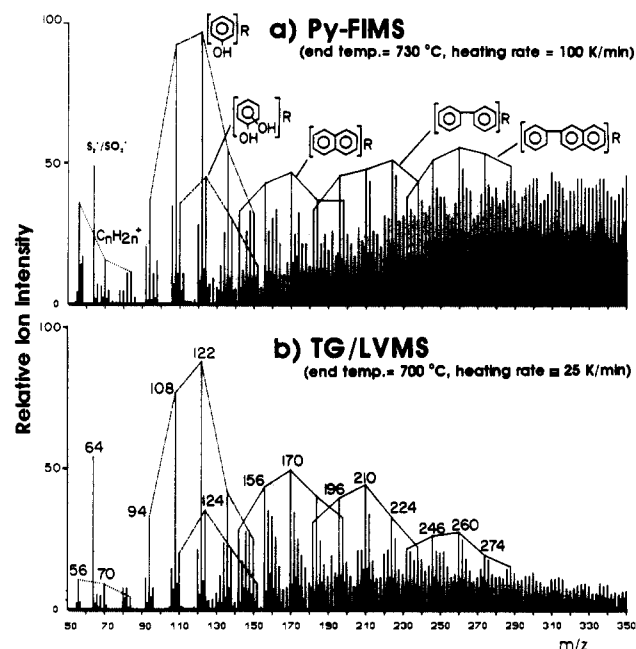


**Figure 6.** Time-integrated spectra obtained by summing all 34 (Py-FIMS) and 40 (TG/LVMS) spectra scanned over the 50–350 amu range.

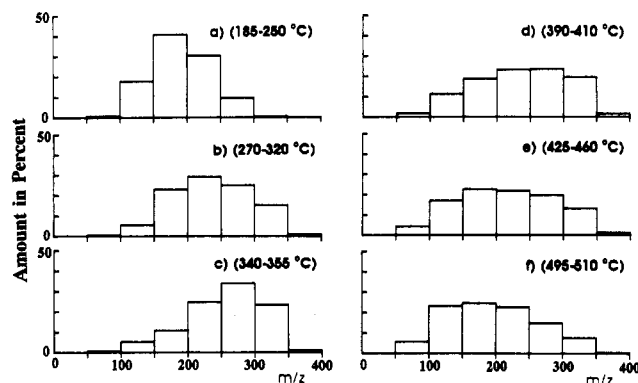


**Figure 7.** Molecular weight distributions of pyrolyzates in six successive temperature intervals during TG/LVMS analysis at 25 K/min.

Py-FIMS TII profile the pyrite decomposition step is obscured by the high peak intensities in the higher mass range versus the relatively low intensity at  $m/z$  64.

When the  $m/z$  50–350 portion of the time-integrated Py-FIMS spectrum is compared with the corresponding TG/LVMS spectrum, as illustrated in Figure 6, highly similar spectral patterns are observed. Because of the ion transmission characteristics of quadrupole mass filters in TG/LVMS, mass intensities are lower in the high mass region compared to those obtained by the magnetic sector instrument used in Py-FIMS. However, with regard to the composition of the pyrolyzates, the same distinct homologous ion series appear to be observed by field ionization and by low-voltage electron ionization, respectively.

MW distributions of pyrolyzates, as observed by TG/LVMS (Figure 7), follow the same trends observed by Py-FIMS (Figure 4). In the low-temperature bitumen desorption step (parts a, b, and c in Figure 7), average MW increases with temperature while average MW decreases with temperature in the bulk pyrolysis step (parts d, e, and f in Figure 7). Because of the increase in average MW with temperature during the bitumen desorption step, the use of low mass range signals only (e.g., 53–193 amu) in Figure 5 results in a different TII profile in which the low-tem-

(25) Yun, Y.; Meuzelaar, H. L. C.; Simmleit, N.; Schulten, H.-R. In *Recent Advances in Coal Science: A Symposium in Remembrance of Peter H. Given*; Schobert, H., Bartle, K., Lynch, L., Eds.; ACS Symposium Series; American Chemical Society: Washington, DC, in press.

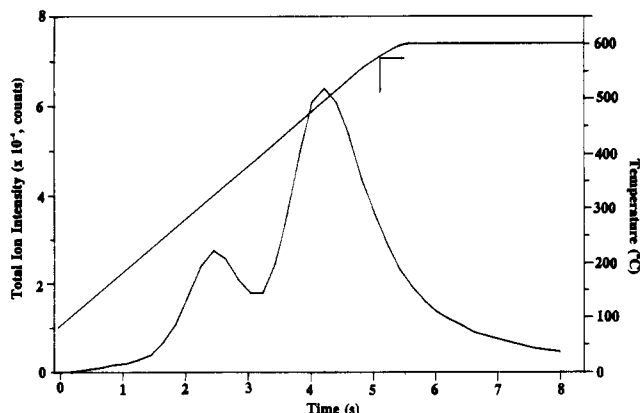


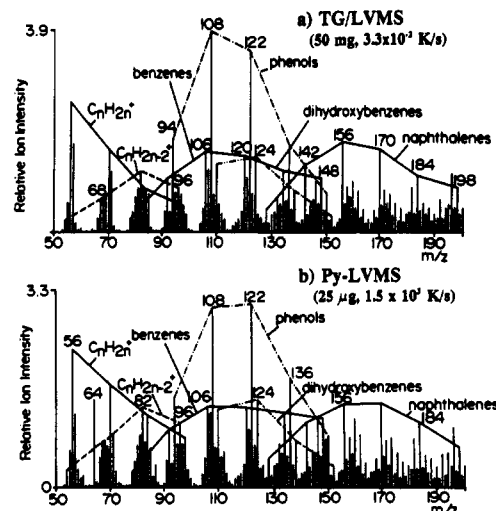
**Figure 8.** Temperature-time profile of blank Curie-point pyrolysis filament (Curie-point temperature 610 °C) superimposed on the total ion intensity profile from Py-LVMS analysis.

perature bitumen evolution peak is completely separated from the bulk pyrolysis event, whereas the inclusion of high mass range signals (Figure 2) results in considerable overlap between the bitumen desorption and bulk pyrolysis peaks.

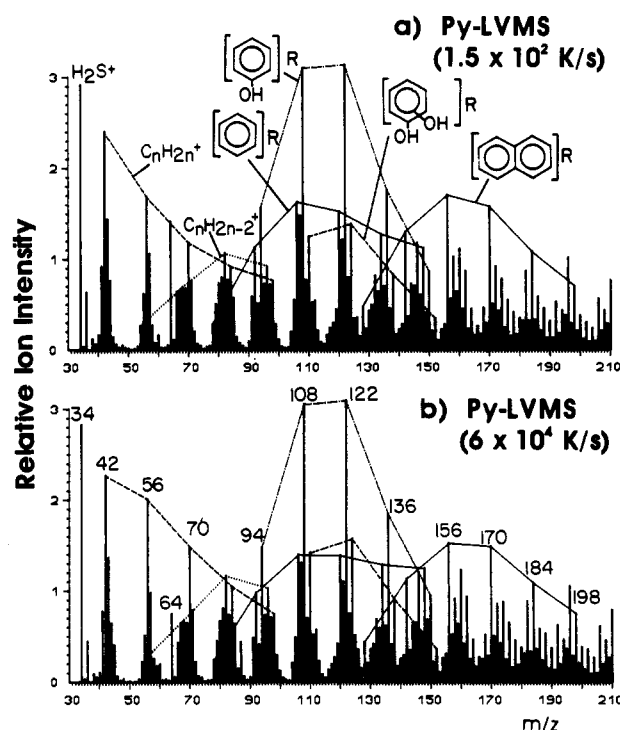
As in Py-FIMS, the MW values observed by TG/LVMS (Figure 7) tend to be more widely distributed in the bulk pyrolysis step than in the bitumen evolution step, although this is not shown as clearly as in Figure 4 due to the mass range limitation of the TG/LVMS experiment.

Figure 8 shows the temperature vs time profile of a blank 610 °C (Curie-point temperature) wire used in Py-LVMS and the corresponding TII profile for Pittsburgh No. 8 coal. A similar bimodal shape is again observed as in Py-FIMS, except for the broader peaks characteristic of the higher heating rate and the more pronounced separation between the bitumen peak and the bulk pyrolysis peak due to the limited mass range ( $m/z$  50–200) scanned, as discussed above. The broadness of the product evolution profiles in Py-LVMS can further be attributed to the effect of diffusion time constants between the pyrolysis zone and the ionization region which is becoming visible because of the much shorter time scale (seconds vs minutes). The relatively high bitumen peak in Py-LVMS as compared to Py-FIMS can be explained by the incomplete devolatilization of some bulk pyrolysis components due to the relatively low final temperature ( $\sim 600$  °C) and by partial loss of some highly polar compounds (e.g., dihydroxybenzenes at  $m/z$  110, 124, 138). The first problem can be overcome by the use of pyrolysis wires with higher Curie-point temperatures whereas the second problem can be minimized by preheating the pyrolysis zone in Py-LVMS runs.<sup>26</sup>

Comparison of TII profiles obtained by TG/LVMS and Py-LVMS reveals three major differences. First, Py-LVMS yields a larger early bitumen peak. Second, the shape of the bulk pyrolysis peak is significantly broadened in Py-LVMS and, third, the pyrite decomposition peak is insignificant in the Py-LVMS data. The explanation for the first and second differences is the same provided for the comparison of the Py-FIMS and Py-LVMS TII profiles, whereas the third difference is due to the different in final end temperatures and heating rates. The final end temperature ( $\sim 600$  °C) used in Py-LVMS is not high enough to cause significant pyrite decomposition during such a short heating time. Moreover, the higher heating rate (approximately 100 K/s) employed in Py-LVMS shifts



**Figure 9.** Time-integrated spectra obtained by summing all 80 (TG/LVMS) and 41 (Py-LVMS) spectra scanned over the 50–200 amu range.



**Figure 10.** Time-integrated spectra obtained by Py-LVMS at two different heating rates.

the decomposition temperature to higher values than observed at the lower TG/LVMS heating rate (25 K/min).

TG/LVMS and Py-LVMS spectra over the 50–200 amu range (Figure 9) show highly similar patterns in which alkyl-substituted phenols ( $m/z$  94, 108, 122, 136) are the most prominent peak series while aliphatic hydrocarbons, as well as alkyl-substituted benzenes, dihydroxybenzenes, and naphthalenes are also represented by strong signals. In order to obtain TG/LVMS spectra at the lowest heating rate (2 K/min), a 50-mg coal sample had to be used in order to produce adequate mass spectrometric signal intensities. Figure 9 compares the integrated spectrum of Pittsburgh No. 8 coal under these conditions with the corresponding Py-LVMS spectrum obtained at much higher heating rate ( $\sim 1.5 \times 10^3$  K/s) while using microgram amounts of sample. Considering a factor of  $4.5 \times 10^4$  difference in heating rate and a factor  $2 \times 10^3$  difference in sample size, as well as the differences in pyrolysis

(26) Taghizadeh, K.; Hardy, R. H.; Davis, B. H. Submitted for publication in *Fuel Processing Technol.*

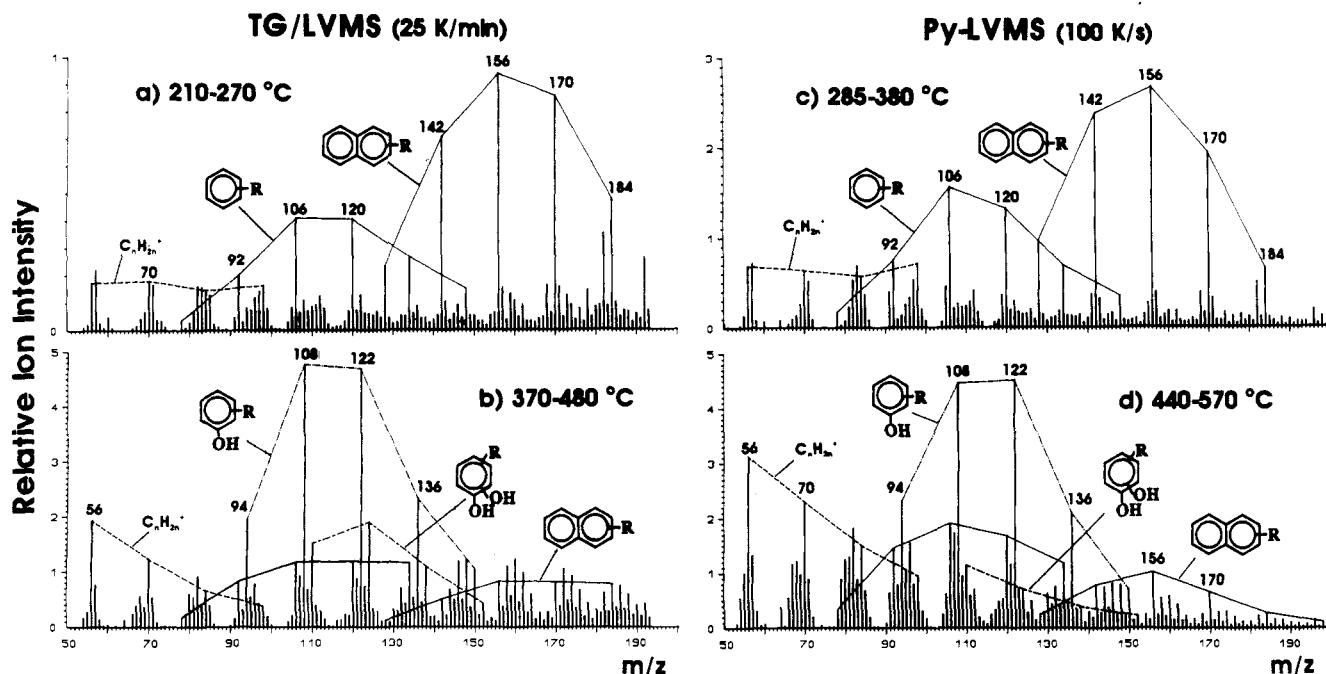


**Figure 11.** Comparison of time-integrated spectra summed at the specific temperature intervals from TG/LVMS (25 K/min) and Py-LVMS (ca. 100 K/s) analyses.

technique, ion source, and type of quadrupole mass filter used, the high degree of similarity with regard to type and relative abundance of the pyrolysis products is quite remarkable. In fact, since Py-LVMS patterns obtained at heating rates of  $6 \times 10^4$  and  $1.5 \times 10^2$  K/s are known to be highly similar as shown in Figure 10, we may conclude that the mechanisms of primary pyrolysis reactions in Pittsburgh No. 8 coal appear to be independent of heating rate over at least 6 orders of magnitude ( $10^{-2}$ – $10^4$  K/s range) when monitoring the 50–200 amu mass range. Moreover, the spectra in Figure 6 suggest that this is also true for higher MW pyrolyzates. However, when comparing the spectra produced by the different techniques, it should be kept in mind that all mass spectra were obtained under high-vacuum ( $<10^{-5}$  Torr) conditions with relatively small particle sizes for the heating rates employed, thus minimizing the effect of mass and heat transport limitations.<sup>6,7</sup>

Figure 11 supplements the conclusion drawn from Figure 9, in that TG/LVMS and Py-LVMS spectra representing the bitumen desorption/distillation steps (Figure 11a,c) as well as the bulk pyrolysis steps (Figure 11b,d) are markedly similar with respect to type and relative abundances of compounds observed by both techniques. The  $T_{\max}$  for each peak in the TG/LVMS and Py-LVMS profiles must be different because of the marked difference in heating rates. As also observed in the Py-FIMS spectra (Figure 3), the  $C_nH_{2n+1}^+/C_nH_{2n}^+$  ratio is higher in the bitumen desorption/distillation step and lower in the bulk pyrolysis step. Moreover, the dominant compound series in the bitumen desorption/distillation step represent alkyl-substituted aromatics as compared to alkyl-substituted hydroxyaromatics in the bulk pyrolysis step.

An interesting observation can be made on the effect of heating the Py-LVMS inlet system by comparing the spectra in Figure 9b and in Figure 11d. The spectrum in Figure 9b was recorded at an inlet temperature of 250 °C whereas that in Figure 11d was obtained at ambient inlet temperature. Low volatile polar components, such as alkyl-substituted dihydroxybenzenes, ( $m/z$  110, 124, 138, 152) are lower in intensity without inlet heating. Also yields of higher MW alkylaromatic series tend to be lower

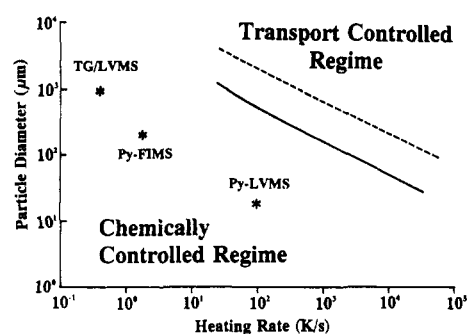


**Figure 12.** Transition from chemical reaction controlled to mass or heat transfer controlled pyrolysis as a function of heating rate and particle size (modified after Howard et al.<sup>7</sup>). Appropriate positions occupied by the three techniques used in our experiments are marked by asterisks (particle diameter parameter estimated from known sample thickness for each technique).

without heating the inlet. These phenomena are mainly due to the inevitable condensation losses of highly polar and/or high MW compounds during transport to the ion source if the inlet system is not preheated properly.

As shown in Figure 5, the 700 °C end temperature of the TG/LVMS experiment is enough to complete the bulk pyrolysis step for which the maximum evolution temperature ( $T_{\max}$ ) was 430 °C. Another noteworthy observation is that  $T_{\max}$  increases with heating rate as predicted by Arrhenius type devolatilization kinetics. For Pittsburgh No. 8 coal at high vacuum ( $<10^{-5}$  Torr),  $T_{\max}$  values were 430, 448, and 495 °C at 25 K/min (from TG/LVMS), 100 K/min (from Py-FIMS), and approximately 100 K/s (from Py-LVMS), respectively. Caution is suggested in the interpretation of  $T_{\max}$  values obtained by vacuum TG/LVMS and Py-FIMS, however, since these do not necessarily represent sample temperatures, but crucible temperatures. In addition, the estimated errors in measured temperatures are  $\pm 10$  °C in TG/LVMS,  $\pm 20$  °C in Py-FIMS, and  $\pm 20$  °C in Py-LVMS. These numbers are mainly associated with the temperature intervals between successive scans.

Furthermore, the effect of heating rate on  $T_{\max}$  has to be interpreted carefully as well since the effect of heat- and



mass-transfer limitations tends to be coupled with heating rate, as illustrated in Figure 12. Nevertheless, based on available literature data,<sup>5,7</sup> heat- and mass-transfer effects are expected to be minimal under the experimental conditions employed here (experiments marked by asterisks in Figure 12). In general, the effects of mass- and heat-transfer limitations are thought to be directly proportional to heating rate, pressure, and particle size (see Figure 12). The Py-FIMS and TG/LVMS analyses reported here employed -100 mesh ANL-PCSP ampule samples. The Py-LVMS experiment used one or two layers of particles of approximately 5–20  $\mu\text{m}$  diameter size by hand grinding a -100 mesh ANL-PCSP ampule sample into a fine suspension in methanol directly before coating the sample on the Curie-point pyrolysis wire. The small particle size and sample layer thickness used in the Py-LVMS runs will tend to minimize the effect of heat and mass transport limitations. However, as indicated in Figure 12, even the larger samples used in Py-FIMS and TG/LVMS pose little threat for transport problems since the larger sample sizes are effectively compensated by the much lower heating rates. Even if the particle diameter is defined in terms of the effective particle diameter after incorporating the effect of multiple particle layers, according to Figure 12 the expected transport problems would seem to be minimal for our experiments. Thus, all spectra discussed until now may be thought to represent primary pyrolysis products without marked effects of mass and heat transport limitations. Consequently, the remarkable constancy of coal pyrolysis profiles obtained under widely varying experimental conditions including many orders of magnitude differences in heating rate and sample size using totally different pyrolysis, ionization, and MS conditions should not be extrapolated to experiments conducted under heat and mass transport limited conditions.

### Conclusions

Time-resolved results from three different vacuum pyrolysis MS techniques reveal that the distribution and the type of the primary pyrolysis products are largely independent of heating rate and of ionization methods. The bimodal TII profiles observed in each experiment and

shown to represent successive evolutions of thermally extractable bitumen and bulk pyrolyzates may explain the relative success of pyrolysis models postulating two parallel routes e.g., Kobayashi's model.<sup>27</sup> Also, the postulation by Anthony et al.<sup>28</sup> that coal pyrolysis occurs through an infinite series of parallel reactions would seem to agree well with the results shown in this paper. However, instead of shifting pyrolysis route due to competitive reactions at increasing heating rate, as proposed by Blik et al.,<sup>6</sup> production of tar components appears to follow relatively independent pathways, at least under high-vacuum conditions where heat and mass transport problems are minimized.

Py-FIMS results indicate that 6–8 wt % (as received) of Pittsburgh No. 8 coal can be attributed to thermally extractable bitumen components. This value lies between typical bitumen yields reported by solvent extraction of toluene (5.7%) and tetrahydrofuran (12.3%), respectively. Thermally extractable bitumen components of Pittsburgh No. 8 coal appear to be mainly of an alkyl-substituted aromatic hydrocarbon nature. With increasing temperature MW distributions tend to become broader during the bitumen evolution step but narrower during the bulk pyrolysis step. These observations support earlier reports by Chakravarty et al.<sup>22</sup> in which the bimodal Py-LVMS profile of Pittsburgh No. 8 coal was explained in terms of sequential distillation and pyrolysis (depolymerization plus thermal degradation) processes, respectively. In the distillation step, lower MW pyrolyzates will evolve first, while during the pyrolysis step, lower MW pyrolyzates will evolve at higher temperatures due to more drastic bond scission processes.

**Acknowledgment.** This work was sponsored by the Advanced Combustion Engineering Research Center. Funds for this center are received from the National Science Foundation, the State of Utah, 23 industrial participants, and the U.S. Department of Energy.

(27) Kobayashi, H.; Howard, J. B.; Sarofim, A. F. *Sixteenth Symposium (International) on Combustion*; The Combustion Institute: Pittsburgh, 1977; pp 411–425.

(28) Anthony, D. B.; Howard, J. B. *AIChE J.* 1976, 22, 625–656.